SUPPORTING INFORMATION

Transforming thymidine into a magnetic resonance imaging probe for monitoring gene expression

Amnon Bar-Shir[1,2], Guanshu Liu[1,3], Yajie Liang[1,2], Nirbhay N. Yadav[1,3], Michael T. McMahon[1,3], Piotr Walczak[1,2], Sridhar Nimmagadda[4], Martin G. Pomper[4], Keri A. Tallman[5], Marc M. Greenberg[5], Peter C.M. van Zijl[1,3], Jeff W.M. Bulte[1,2,6,7], and Assaf A. Gilad[1,2,3*].

[1] Division of MR Research, Russell H. Morgan Department of Radiology, The Johns Hopkins University School of Medicine, Baltimore, MD, United States

[2] Cellular Imaging Section, Institute for Cell Engineering, The Johns Hopkins University School of Medicine, Baltimore, MD, United States

[3] F.M. Kirby Research Center for Functional Brain Imaging, Kennedy Krieger Institute, Baltimore, MD, United States

[4] Russell H. Morgan Department of Radiology, The Johns Hopkins University School of Medicine, Baltimore, MD, United States

[5] Department of Chemistry, The Johns Hopkins University, Baltimore, MD, United States

[6] Department of Biomedical Engineering, The Johns Hopkins University, Baltimore, MD, United States

[7] Department of Chemical & Biomolecular Engineering, The Johns Hopkins University, MD, United States

***Corresponding author:** Assaf A. Gilad, Ph.D., The Johns Hopkins University School of Medicine, 1550 Orleans St., Cancer Research Building II, Room 4M63, Baltimore, MD 21231. Phone: 410-502-8188, Fax: 410-614-1948, Email: assaf.gilad@jhu.edu.

Supporting Information Methods

Simulations of CEST data: CEST data were simulated using the Bloch equations for a four-pool model[1,2] consisting of an imino NH proton, two hydroxyl protons, and bulk water protons for dT, **1**, **2** and **3**. Simulation parameters were determined from fitting the Bloch equations to CEST experimental data at 11.7 Tesla (Manuscript, Figure 1 c-e). For convenience, other pools were simulated with the same relaxation parameters. Exchange parameters for each pool were determined from QUESP experiments (Manuscript, Figure 1 g-j and Table 1). The simulations were performed for two different magnetic field strengths, 11.7 Tesla and 3.0 Tesla with an 8 s, 4 μT continuous wave (CW) CEST pulse.

***In vitro* imaging using a clinical 3 Tesla MRI scanner**: Experiments were performed on a 3.0 Tesla Philips Achieva system (Philips Healthcare, Best, The Netherlands) using a body coil for transmit and a small animal solenoid coil for reception. CEST data were collected using a pulsed acquisition scheme[3] with a 25 ms, 164 Hz frequency selective saturation pulse followed by a partial EPI readout (EPI factor 3). This TR interval was repeated until a 3D volume was acquired with 5 slices (slice thickness of 10 mm) across a field of view of 48 × 45 mm^2 (in plane resolution of 0.75 mm × 0.9 mm). The acquisition per irradiation frequency consisted of TR/TE = 65/5.5 ms and 4 averages. A total of 64 images were acquired which included an unsaturated volume and 63 saturated volumes with equally spaced frequency offsets between ± 10 ppm (relative to the water frequency). The total acquisition time was 26 min 38 s. The experiments for B_0 correction[4] were run the same except that 40Hz frequency selective saturation pulse was used. Data processing was performed as described in *Experimental section* (manuscript).

Cell Viability Assay: Cell viability assay was performed using CellTiter-Blue® Cell Viability Assay (Promega), which provides a fluorometric method for estimating the number of viable cells present in 96 well plate. HEK293FT cells transduced with the HSV1-*tk* ($293^{HSV1\text{-}tk}$) were plated in 96 well-plate (10,000 cells/ well). Cells were incubated for a periods of 4 hours and 24 hours in the presence of ganciclovir (GCV, 0.5mg/ml in cell medium), compound **2** (0.5mg/ml in cell medium) and medium (as control). CellTiter-Blue® Reagent was added (20μl/well) and plate was incubated for 3 hours at 37ºC. Finally, fluorescence 560/590nm was recorded and values obtained from

probe containing wells (GCV or **2**, N=4) were normalized to values of non-treated cells (control wells) to determine the % of viable cells after the incubation period.

In vitro uptake assay: One million cells ($9L^{wt}$ and $9L^{HSV1\text{-}tk}$ in triplicates) were incubated in 200ml medium containing 1μCi [^{125}I]FIAU at 37°C for 1 and 3 h. Cells were pelleted by centrifugation and washed 3 times with cold PBS. Gamma counter was used to monitor the radioactivity of the incubating medium and the incubated cells. [^{125}I]FIAU uptake was determined as the relative radioactivity (in percentage) of the cells to that of the incubating [^{125}I]FIAU medium (without cells).

***In vivo* CEST-MRI (full CEST-spectrum)**: At the last time point of the experiment the full CEST-spectrum was acquired for each animal with the same parameters described in the Experimental Section (main text) except the followings: CEST-weighted images were acquired with a modified RARE pulse sequence (TR/TE = 6000/35ms), using a 213Hz/4000ms saturation pulse from -6 to +6 ppm around the water resonance, which was assigned to be at 0 ppm. Pixel-based B_0 correction was used as described before[4] using the same parameters as above except for TR=1500 ms, B_1/t_{sat} = 21 Hz/500ms, with a sweep range from -1 to +1 ppm (0.1 ppm steps). Mean CEST spectra were plotted from an ROI for each tumor and normal brain tissue, after B_0 correction. $MTR_{asym}=100\times(S^{-\Delta\omega} - S^{\Delta\omega})/S_0$ was computed at different offsets Δω.

Terminal Transferase nick-end-labeling (TUNEL): ApopTag® Plus In Situ Apoptosis Fluorescein Detection Kit (Millipore) was used for detecting degraded DNA fragments to evaluate apoptosis after the administration of compound **2**. Six hours after i.v. administration of **2** (150mg/kg body weight) mice were transcardially perfused with 10 mM PBS and 4% PFA for tissue fixation. Brains were fixed in 4% PFA overnight, cryopreserved in 30% sucrose, and followed by cryo-sectioning at 30 μm slices. Slices were post-fixed in ethanol: acetic acid (2:1) solution followed by the manufacture procedure for using the ApopTag® Plus *In Situ* Apoptosis Fluorescein Detection Kit (Millipore, S7111).

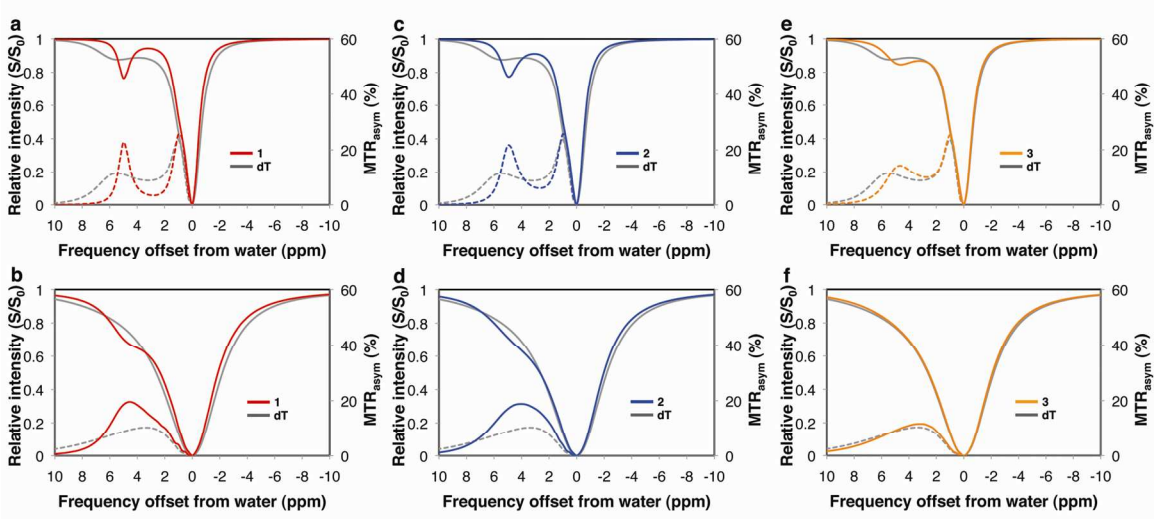

Figure S1. Simulation of CEST spectra and MTR_{asym} plots at different magnetic field. Simulated CEST-spectra (solid lines) and MTR_{asym} plots (dashed lines) of dT (gray, a-f), **1** (red, a-b), **2** (blue, c-d) and **3** (orange, e-f). Panels a (dT vs. **1**), c (dT vs. **2**) and e (dT vs. **3**) represent the simulated CEST data for MRI scanner operating at 11.7 Tesla magnetic field. Panels b (dT vs. **1**), d (dT vs. **2**) and f (dT vs. **3**) represent the simulated CEST data for MRI scanner operating at 3 Tesla magnetic field.

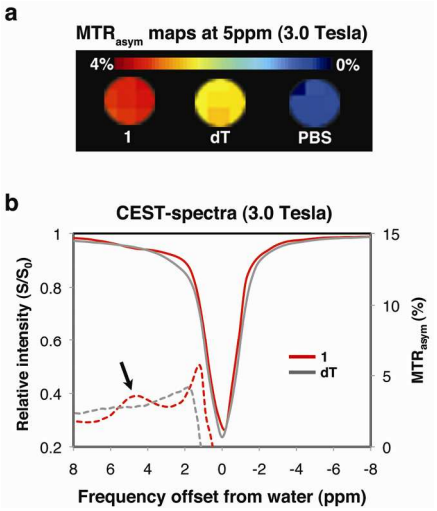

Figure S2. **CEST imaging obtained at 3.0 Tesla clinical MRI scanner.** a) MTR_{asym} maps of PBS, dT, and **1,** obtained at a 5ppm frequency offset from the water resonance. b) CEST-spectra (solid lines) and MTR_{asym} plots (dashed lines) of dT (gray) and **1** (red). Arrow points to the maximal MTR_{asym} obtained from the imino proton of **1**. CEST data were acquired for 20 mM CEST-agent (pH=7.4) at room temperature at 3.0 Tesla (B_1=164 Hz) MRI scanner.

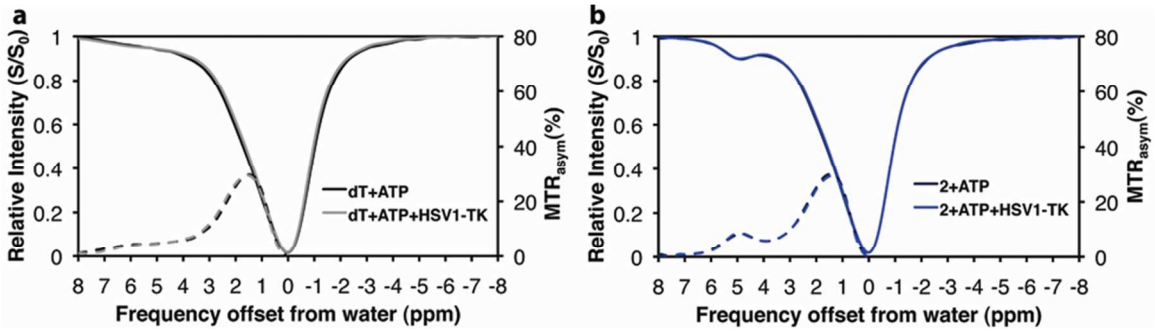

Figure S3. **Phosphorylation effect on CEST data**. CEST-spectra and MTR_{asym} plots obtained for the thymidine kinase reactions (phosphorylation) with and without purified recombinant HSV1-TK enzyme for either dT (a) or analog **2** (b) as CEST substrates. Note that the lines are overlapping, indicating no change is the CEST contrast after phosphorylation.

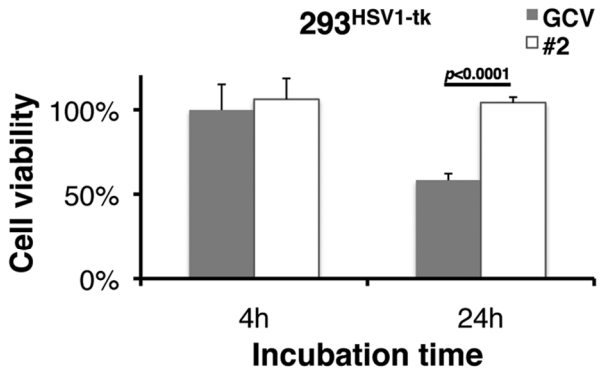

Figure S4. **Cell viability assay**. Cell viability assessment of 293FT cells, transduced with HSV1-*tk* gene ($293^{HSV1\text{-}tk}$). $293^{HSV1\text{-}tk}$ cells were incubated with 0.5mg/ml of either Ganciclovir (GCV) or compound **2** for 4 and 24 hours. Cell viability was determined as a percentage of treated cells compare to untreated $293^{HSV1\text{-}TK}$ cells (100%). Note that **2** had no toxic effect on the cells while GVC killed about 50% of the cells after 24 hour.

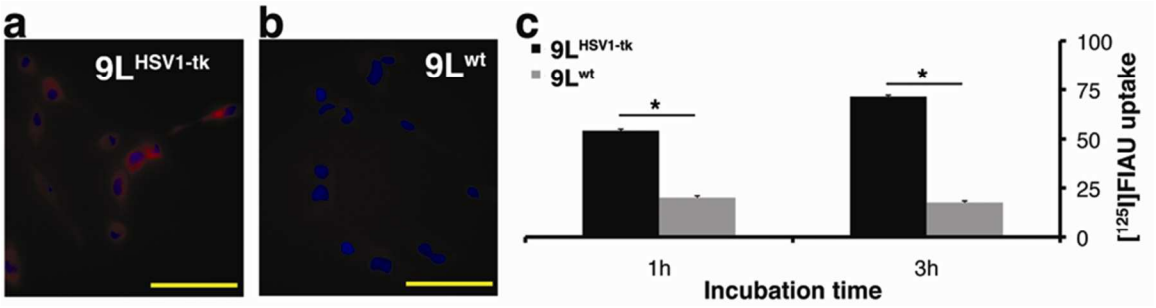

Figure S5. Expression and activity of HSV1-TK in 9L-rat glioma cells. Immunofluorescence of a) $9L^{HSV1\text{-}tk}$ and b) $9L^{wt}$ cells using anti-V5 antibody (red) for HSV1-TK staining overlaid on a DAPI staining (blue), bar=50μm. c) percentage of [^{125}I]FIAU uptake by control ($9L^{wt}$) cells and cells stably expressing the HSV1-TK ($9L^{HSV1\text{-}tk}$) after 1h and 3h incubation with 1μCi [^{125}I]FIAU. * $p< 5\times10^{-9}$ (student's t-test, unpaired, two-tailed).

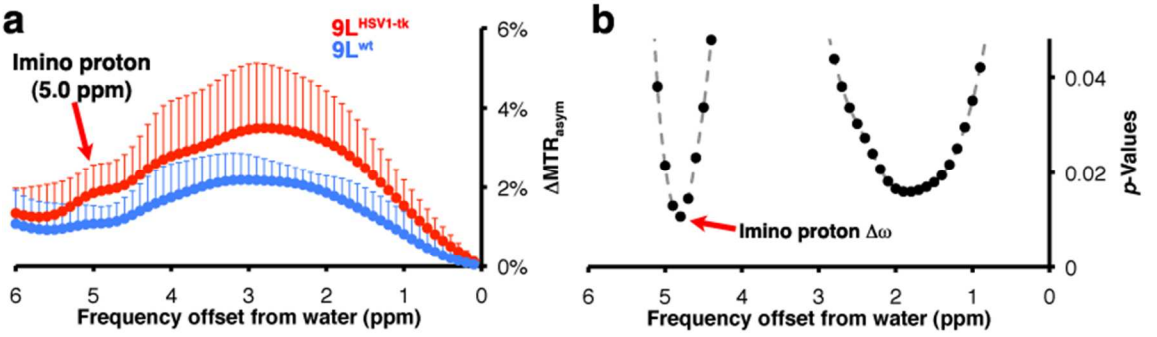

Figure S6. ***In vivo*** **detection of the imino proton in $9L^{HSV1\text{-}tk}$**. a) ΔMTR_{asym} plots of $9L^{wt}$ (blue) and $9L^{HSV1\text{-}tk}$ (red) (mean ± s.d.; N=8 mice). The arrow pointing to the local maximal ΔMTR_{asym} represents the imino proton at 5 ppm after accumulation of **2** in $9L^{HSV1\text{-}tk}$ tumor. MTR_{asym} ($MTR_{asym}=100\times[S^{-\Delta\omega} - S^{\Delta\omega}]/S_0$) was calculated from a complete CEST-spectrum (from -6 ppm to + 6 ppm; S_0 image without saturation). b) P-values for each Δω (Student's t-test, unpaired, two-tailed) comparing the ΔMTR_{asym} of $9L^{wt}$ or $9L^{HSV1\text{-}tk}$ tumors. The lowest *p*-value was obtained at 5 ppm frequency offset from water (red arrow), as expected due to the accumulation of **2** solely in $9L^{HSV1\text{-}tk}$. Note that second set of significant differences (*p*-values<0.05) between the two tumor type was found at the frequency of the hydroxyl protons (compare with MTR_{asym} plot at Figure S1 b). In these frequencies, however, the signal is more affected by direct water saturation and the asymmetry of the conventional MT[5].

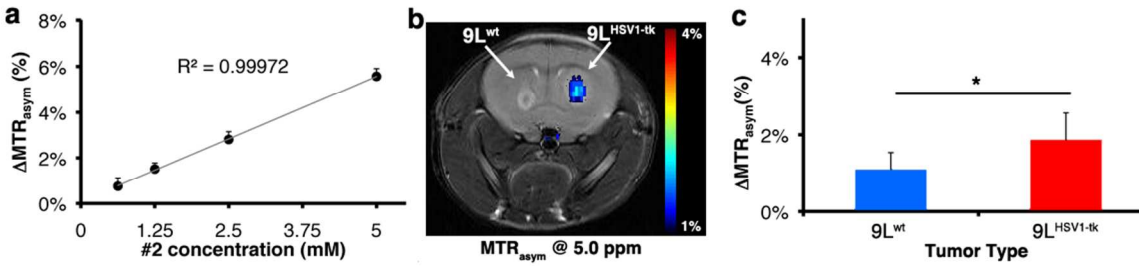

Figure S7. Estimation of 2 accumulation in HSV1-tk expressing cells *in vivo*. a) Calibration curve; ΔMTR_{asym} values (at $\Delta\omega$=5.0 ppm) as a function of **2** concentration (mM) in PBS (11.7 Tesla, B_1=170Hz/4000ms, pH=7.4, and 37ºC, R^2=0.9997). b) Representative *in vivo* MTR_{asym} (5.0 ppm) map of the mouse brain overlaid on T_2-weighted images, showing the distribution of **2** at the last experimental time point. c) The calculated ΔMTR_{asym} values based on the CEST spectra MTR_{asym} ($100\times[S^{-5ppm} - S^{5ppm}]/S_0$; mean ± s.d.; N=8 mice) at 5.0 ppm for each tumor after accumulation of **2** (* *p*-value<0.05). The average difference between the two tumor types was approximately 0.77% (N=8, *p*-value=0.021). Using the calibration curve the estimated intracellular concentration of **2** is approximately 0.7 mM. The same concentration was found from simulating CEST data using the Bloch equations as described above in the Supporting Information Methods section.

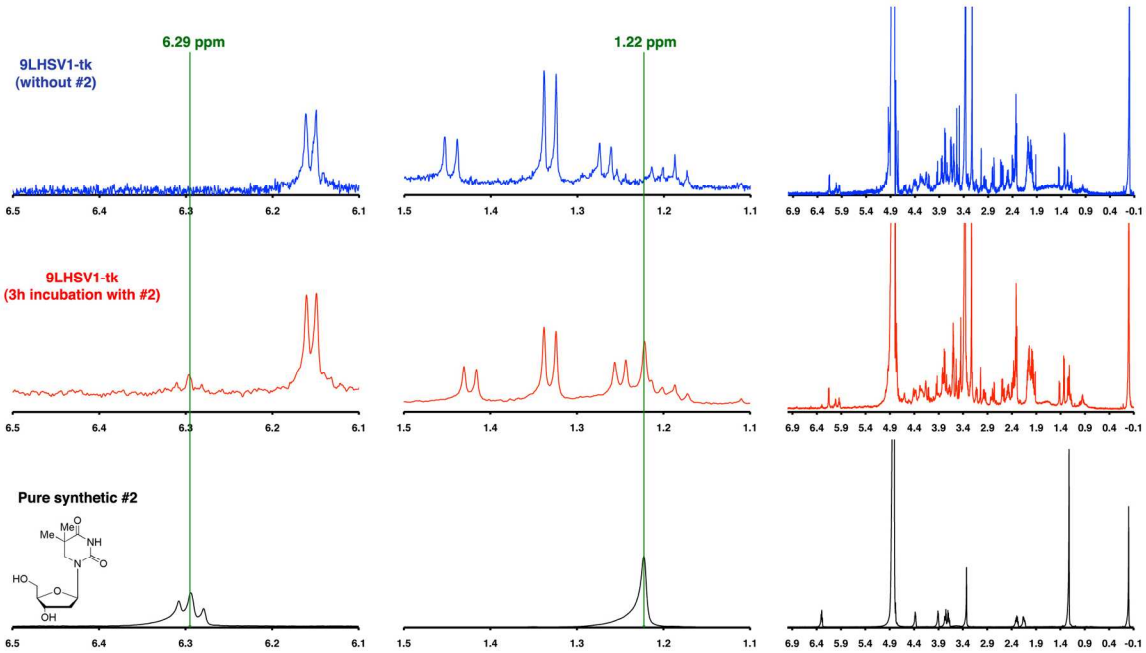

Figure S8. In vitro detection of 2 accumulation with MR spectroscopy. At least two distinctive peaks, typical to **2**, appear in the spectra of the pure compound (black), a singlet at 1.22 ppm (6H of the 2 Methyls) and a triplet at 6.29 ppm (1H , the proton on 1' carbon of the sugar). Both peaks appear in the lysate of cells incubated with the compound (red spectra) but not in the control (blue spectra). The samples were prepared using dual-phase extraction for simultaneous extraction of cellular lipids and water-soluble metabolite[6]. Twenty five million cells ($9L^{HSV1\text{-}tk}$) were incubated with or without **2** for 3.5h. After dual-phase extraction and lyophilizing of the water from the water-soluble fraction, the soluble intracellular contents were dissolved in D_2O for the ^{1}H-NMR experiments. Fully relaxed ^{1}H-NMR spectra of the extracts were acquired on a Bruker 500MHz scanner. The signal integrals of the typical functional groups of **2** (methyl groups -$(CH3)_2$ at 1.22 ppm and of the CH on the C-1' position of the sugar moiety at 6.29 ppm) and of the standard TSP (0 ppm) were determined. Then, the mM intracellular concentration of **2** was calculated as shown previously[6] and found to be 0.37mM.

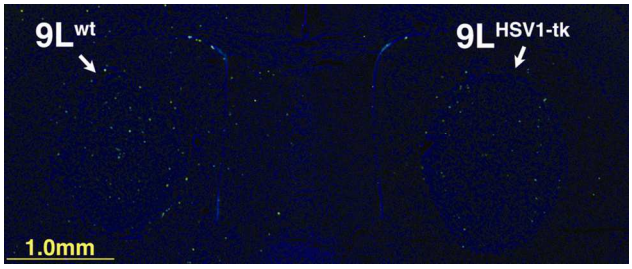

Figure S9. **Apoptosis assessment**. Monitoring apoptotic cells using TUNEL staining. Fixed brain of mouse injected with **2** (150mg/kg body weight; 6 hours post i.v. injection) revealed very few apoptotic cells (green, overlaid on blue, DAPI staining) in both tumors (either $9L^{wt}$ or $9L^{HSV1\text{-}tk}$). Thus, demonstrating that **2** do not induce apoptosis *in vivo*.

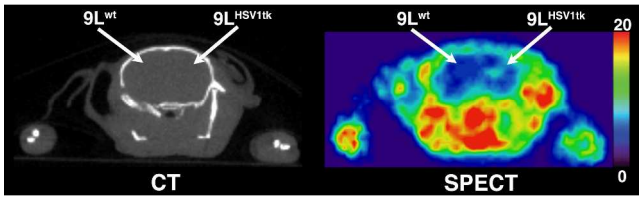

Figure S10. Raw images (transverse views) of CT (left panel) and SPECT (right panel) obtained three hours after i.v. injection of [^{125}I]FIAU. Left hemisphere: wild type 9L tumor ($9L^{wt}$); right hemisphere: 9L tumor expressing HSV1-TK ($9L^{HSV1\text{-}tk}$).

References

(1) Woessner, D. E.; Zhang, S.; Merritt, M. E.; Sherry, A. D. *Magn. Reson. Med.* **2005**, *53*, 790.

(2) Li, A. X.; Hudson, R. H.; Barrett, J. W.; Jones, C. K.; Pasternak, S. H.; Bartha, R. *Magnetic resonance in medicine : official journal of the Society of Magnetic Resonance in Medicine / Society of Magnetic Resonance in Medicine* **2008**, *60*, 1197.

(3) Jones, C. K.; Polders, D.; Hua, J.; Zhu, H.; Hoogduin, H. J.; Zhou, J.; Luijten, P.; van Zijl, P. C. *Magn Reson Med* **2011**.

(4) Kim, M.; Gillen, J.; Landman, B. A.; Zhou, J.; van Zijl, P. C. *Magn Reson Med* **2009**, *61*, 1441.

(5) van Zijl, P. C.; Yadav, N. N. *Magn Reson Med* **2011**, *65*, 927.

(6) Glunde, K.; Raman, V.; Mori, N.; Bhujwalla, Z. M. *Cancer Res* **2005**, *65*, 11034.